Energy &
Environment Nexus

https://doi.org/10.48130/een-0026-0021

Original Research

Open Access

End-of-life tire-derived carbon as an alternative carbon source for electric arc furnace steelmaking

Yanghao Jin[1#], Yazhe Wang[1#], Zexuan Li[1], Samina Gulshan[1], Tong Han[1], Aekjuthon Phounglamcheik[2], Konstantinos Rigas[2], Ziyi Shi[1*], Pär G. Jönsson[1] and Weihong Yang[1]

Received: 16 July 2026

Revised: 25 August 2026

Accepted: 8 October 2026

Published online: 10 November 2026

Abstract

Compared with the traditional blast furnace-based steelmaking industry, electrification in steelmaking is revolutionizing this field. Electric arc furnace (EAF) steelmaking is a typical process, and it can significantly reduce greenhouse gas emissions. However, even in the EAF, fossil-based carbon materials consumption is still a challenge for decarbonization in the steelmaking industry. As a renewable alternative carbon source, practical use of biocarbon is hindered by technical limitations and economic constraints. This study focuses on the potential of tire-derived carbon (TC) as a sustainable and economically attractive alternative carbon source (ACS) for the EAF process. Pyrolysis parameters of tire were first investigated at a temperature range between 500 and 700 °C. Secondly, the washing treatment using HCl combined with H_2O_2 for desulfurization was evaluated, successfully reducing sulfur to an acceptable level (0.37 wt.%) and also significantly decreasing other undesired impurities such as phosphorus. Based on the comparative analysis of Raman, XRD, and BET, the results showed that desulfurized TC has a similar structure to conventional metallurgical carbon. Furthermore, a detailed techno-economic analysis demonstrated that TC production is economically favorable, achieving significantly lower production costs compared with biocarbon. This work clearly established TC as an economically competitive, technically beneficial, and technically feasible ACS, effectively supporting the steel industry's transition toward enhanced resource circularity and reducing fossil fuel dependency.

Keywords: End-of-life tires, Electric arc furnace steelmaking, Pyrolysis, Desulfurization, Alternative carbon source, Techno-economic analysis, Circular economy

Highlights

- Pyrolysis converts end-of-life tires into carbon-rich solids suitable for EAF.
- Desulfurization with HCl + H_2O_2 reduced sulfur in tire carbon to 0.37 wt.%.
- Tire-derived carbon shows structural similarity to metallurgical coke after treatment.
- Techno-economic analysis reveals tire-carbon is cost-competitive and viable.
- Valorizing waste tires supports circular economy and cleaner steel production.

# Authors contributed equally: Yanghao Jin and Yazhe Wang

* Correspondence: Ziyi Shi (ziyis@kth.se)

Full list of author information is available at the end of the article.

https://doi.org/10.48130/een-0026-0021

Graphical abstract

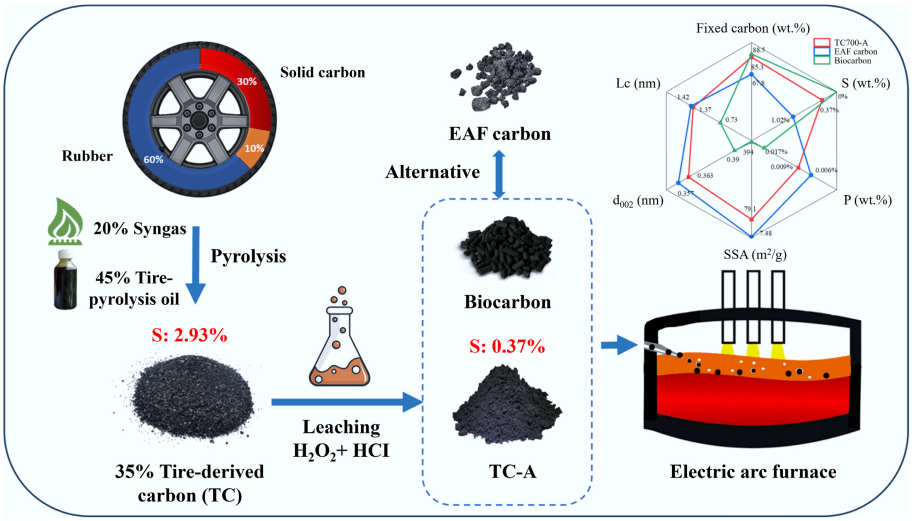

Introduction

The steel industry accounts for about 7% of the total global CO_2 emissions, as the International Energy Agency (IEA) reported in 2020[1]. According to the net-zero emissions in industry by 2050, the whole steel industry is looking for a more sustainable production process[2]. The electric arc furnace (EAF) process is an optimal option, which primarily uses recycled steel scrap and renewable electricity that can reduce CO_2 emissions[3]. Specifically, it emits approximately 0.3 tons of CO_2 per ton of steel, compared with around 2.3 tons from the conventional blast furnace-basic oxygen furnace (BF-BOF) process, and significantly reduces impacts across other environmental categories[4]. In Europe, the EAF share of the total steel production has reached 44.8%; meanwhile, it contributes around 15%–20% of the steel industry's carbon emissions, marking its environmentally friendly advantage[5]. Some European countries, notably Sweden, are targeted to achieve 100% fossil-free steel production by 2045. In this context, EAF in steelmaking is recognized as a main and suitable pathway for aiding decarbonization[6].

Even though EAF already reduces CO_2 emissions, it still consumes carbon-based materials, which are used as the reductant and electrodes in the process. In this context, this operation typically consumes around 12 kg of carbon per ton of steel[7]. These carbon materials in EAFs are still derived from fossil fuels, and this is why the EAF also emits CO_2[8]. Although the quantity of carbon consumption is relatively low compared with BF-BOF processes, fossil-derived carbons are still a major contributor, occupying approximately 40%–70% of direct CO_2 emissions from EAF steelmaking[7]. This reveals a critical gap in achieving the truly sustainable and carbon-neutral target of steel production through EAF routes; therefore, it is necessary to look for sustainable alternative carbon sources (ACS)[9].

Among ACS candidates, biomass-derived biocarbon has been widely studied and shown technical potential in the past 10 years[10,11]. Both laboratory and industrial experiments have demonstrated that biocarbon can effectively be considered to replace portions of fossil-based carbons without causing damaging effects on furnace or steel quality[12,13]. However, biocarbon itself still presents several application limitations. It usually exhibits high CO_2 reactivity, poor wettability, and high phosphorus content. All of these make its direct use in EAF processes difficult and demand an additional agglomeration process[14]. Additionally, the economic viability of biocarbon remains repressed by other considerations, such as its high production costs (approximately US$500–600 per ton[15]), limited biomass availability, seasonal variability[16], and strong competition for biomass resources from multiple industries[17]. These factors pose technical, economic, and logistical challenges that currently hinder the large-scale implementation and industrial adoption of biocarbon as a sustainable ACS solution.

Compared with biomass, end-of-life (EOL) tires represent a compelling raw material for an alternative carbon source. Globally, approximately 1.5 billion tons used tires are discarded each year, creating a massive, continuous waste stream that also causes significant environmental harm[18]. In Europe, around 3.58 million tons of EOL tires were generated in 2018, with 91% collected and predominantly processed through material recovery and energy recovery routes[19]. Compared to biomass, these EOL tires benefit from a mature centralized collection system and a stable supply, resulting in lower costs when used as an ACS[20]. Despite these advantages, EOL tires possess high volatile matter content, low carbon content, and high sulfur levels, rendering them unsuitable for direct use in EAFs. Consequently, they can only be utilized in EAFs when co-injected with metallurgical coke.

Pyrolysis is a thermochemical conversion process that transforms organic waste into high-value products. This process transforms EOL tires into a carbon product with high carbon content and low volatile matter, making its properties better suited for EAF applications. Additionally, the process yields high-value byproducts, such as pyrolysis oil and non-condensable gases. However, sulfur deposition during pyrolysis typically raises the sulfur content of EOL tire-derived carbon (TC) to 1.5 wt.%–3.5 wt.%, which exceeds the < 1 wt.% threshold tolerated in steelmaking because of the risk of product degradation[21]. Consequently, efficient desulfurization is essential, but only very few studies have explored the use of TC in EAF steelmaking. Previous studies on the desulfurization of TC have mainly focused on producing high-quality recovered carbon black (rCB), involving complex and economically intensive purification processes[22,23]. Such methods are not economically achievable or suitable for EAF steelmaking, which demands lower-cost, simpler,

yet effective desulfurization strategies. Additionally, detailed comparative analyses of the physicochemical properties and reactivity of TC relative to both commercial EAF carbon and emerging biocarbon are critically lacking in the literature. Systematic techno-economic assessments (TEA) evaluating TC as a cost-effective ACS specifically for EAF steelmaking applications have not yet been comprehensively conducted.

Therefore, this study focuses on the potential of TC as an ACS for EAF steelmaking. Firstly, the feasibility of producing TC by pyrolysis was evaluated, and then an HCl/H_2O_2 desulfurization process was applied to ensure that the TC samples could meet the requirements for carbon materials used in EAF steelmaking. Compared with previous studies, this work centered on reducing the sulfur and phosphorus content of TC samples to reach the standards of EAF steelmaking. Additionally, the applicability of TC for EAF steelmaking was evaluated by comparing TC samples with biocarbon and commercial EAF carbon, while also analyzing differences in their physicochemical properties. Furthermore, a techno-economic analysis (TEA) was conducted to assess the economic competitiveness of these production and desulfurization processes. This study aimed to evaluate whether TC samples can replace the commercial fossil-based coke as a technically feasible and economically attractive substitute in the EAF process, thereby promoting resource recycling and reducing CO_2 emissions in steelmaking. This research mainly focuses on the pyrolysis and desulfurization processes and characterization of TC. This lays an experimental foundation for following stages involving briquetting/granulation, pilot-scale EAF testing, and process integration between EOL tire pyrolysis and steelmaking production.

Methodology

A schematic overview of the research methodology in this study is presented in Fig. 1. First, preliminary thermogravimetric analysis (TGA) and elemental analyses were conducted on EOL tires to determine their basic physical and chemical characteristics. Based on these results, an optimal temperature range was selected for pyrolysis experiments. These pyrolysis experiments produced gaseous, liquid, and carbon products, which were characterized to boost and optimize the process and to establish a foundation for following systematic analysis. Moreover, energy and mass balance evaluations and the selected carbon production parameters were applied to TEA to evaluate the technological and economic potential of the pyrolysis process. The detailed description of the samples and characterization methods used in this study is illustrated in the following parts.

Raw materials

The EOL tires used in this study were provided by Stena AB (Sweden), as shown in Supplementary Fig. S1. Their proximate and ultimate properties are presented in Supplementary Table S1, while the detailed ash content is shown in Supplementary Table S2. For comparison, a reference biocarbon was provided by Envigas AB (Sweden), and a commercial EAF carbon sample was obtained from a steelmaking company. Biocarbon was produced from softwood pellets through pyrolysis at approximately 600 °C. The size of this biocarbon is around 1 cm. This biocarbon has been applied for testing at an EAF plant previously, and therefore, it was selected as a bio-based reference. The commercial EAF carbon, supplied by a steelmaking company participating in this work, was chosen as the commercial fossil-carbon reference, and its tough lump size is about 5 cm. Hydrochloric acid (HCl) and hydrogen peroxide (H_2O_2) were ACS-grade reagents purchased from Sigma-Aldrich.

Pyrolysis experiments

The pyrolysis experiments were conducted in a vertical tube furnace (KJ-T1400-60IIC, from Zhengzhou KJ Technology Co., Ltd, China). For each experiment, 30 g of tire pieces were placed in the middle of the furnace in a 316 L stainless steel crucible. During the heat-up stage, the temperature increased at 20 °C/min; the samples were then maintained at target pyrolysis temperatures of 500, 600, and 700 °C for 1 h. To accurately measure the sample temperature, a thermocouple was placed inside the crucible in direct contact with the material. During pyrolysis, the volatiles first passed through three condensers, which were immersed in a cooling bath at −10 °C. These condensable vapors were collected as liquid side products after the experiments for further characterization, and these liquid products were named

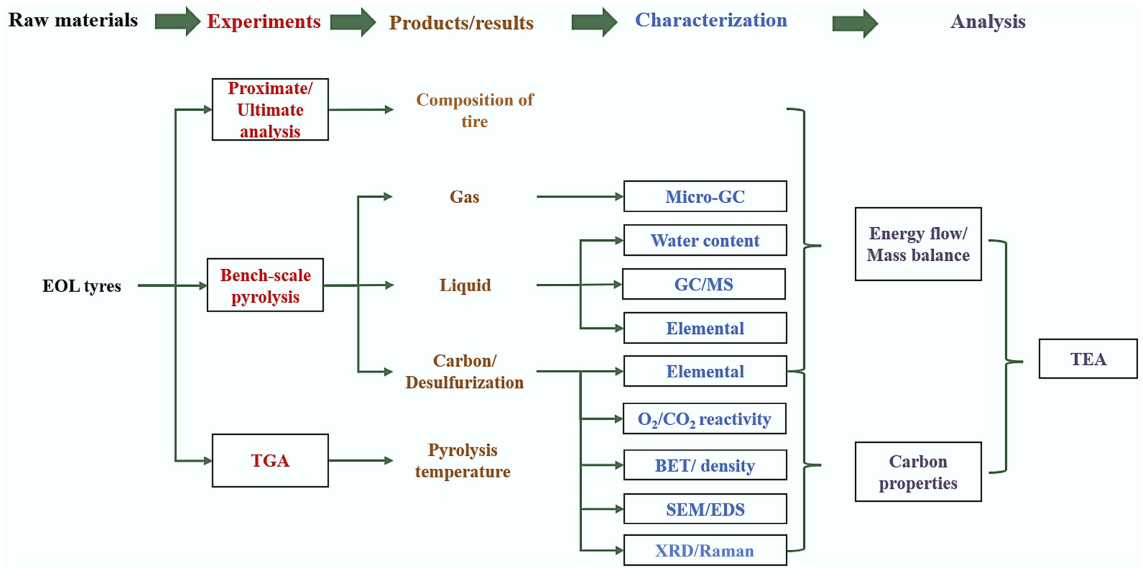

Fig. 1 Experimental procedure of TC for EAF.

https://doi.org/10.48130/een-0026-0021

tire-pyrolysis oil (TPO). The non-condensable gases (NCG) were carried by nitrogen, which was the protective gas, and passed through a 490 Micro GC instrument for online measurements of the gas composition, and the total gas volume was recorded with a gas meter (TG3/5–50 mbar, from RITTER Apparatebau GmbH and Co. KG, Germany). The remaining NCG were collected in gas bags for further compositional analysis. After the reactor had cooled down to room temperature, the TC was collected from the crucible. These TC samples obtained at different pyrolysis temperatures were designated as TC500, TC600, and TC700.

Desulfurization experiments

Desulfurization experiments were conducted using HCl in combination with H_2O_2 as the oxidizing agent. The types of desulfurizing agents and their corresponding agent-to-carbon ratios are summarized in Supplementary Table S3.

Approximately 200 mL of the acid or acid-oxidizing agent solution was added to a 600 mL beaker containing 5 g of TC. The mixture was stirred and maintained at 60 °C for 12 h. Afterward, the solid residue was separated by vacuum filtration and thoroughly rinsed with deionized water until its pH reached neutrality. Finally, the desulfurized TC was dried in an oven at 110 °C overnight to obtain the purified and de-moisturized solid product.

Characterization methods

Characterization of raw materials

TGA of the EOL tire sample was performed on a Mettler TGA/DSC 3^+ STARe system, equipped with a Huber minichiller 600 cooler. Approximately 10 mg of EOL tire sample was placed into a 100 μL aluminum cup. The sample was heated from 25 to 800 °C at a rate of 20 °C/min under an N_2 flow of 50 mL/min and then held at the final temperature for 1 h.

The ultimate composition and proximate analyses, including the moisture, fixed carbon, volatile matter, and ash contents of EOL tire, were tested by Eurofins Biofuel and Energy Testing Sweden AB (Sweden).

Characterization of carbon materials

The O_2/CO_2 reactivity tests were conducted using a Mettler TGA/DSC 3^+ STARe system, equipped with a Huber minichiller 600 cooler. A 10 mg TC sample was placed into 100 μL aluminum crucibles. For the O_2 reactivity test, the TC sample was heated from 30 to 525 °C at a heating rate of 30 °C/min under a flow of 50 mL min^{-1} N_2 as the protective gas. When the target temperature was reached, the gas was switched to O_2 at the same flow rate, and the sample was held under these conditions for 3 h. For the CO_2 reactivity test, the carbon sample was heated to 960 °C at a rate of 20 °C/min under a nitrogen flow of 100 mL/min. After maintaining the target temperature for 10 min, the gas was switched to CO_2 at the same flow rate, and the sample was held for 3 h.

The ultimate compositions of TC samples were determined using a 'vario MICRO cube' elemental combustion analyzer. The oxygen content in all cases was determined by difference (100%−C%−H%−N%−S%) on a dry basis. The proximate analysis of TC samples was tested by Shiyanjia (China) following the GB/T 212-2008 standard.

Morphological characteristics were examined by a Thermo Fisher Scientific Apreo 2s LoVac field-emission scanning electron microscope (SEM). This instrument was equipped with an Ultradry 60 mm^2 energy-dispersive X-ray spectroscopy (EDS) detector, which enabled integrated EDS mapping (ChemiSEM) within the SEM software.

The carbon structure information of the samples was evaluated by an X-ray diffraction (XRD, PANalytical X'Pert Pro), which is equipped with a Cu K_α source operating at 30 kV and 15 mA. The scanning range of the Bragg angle (2θ) was set between 10° and 80°, with a step size of 0.05°. The interlayer spacing of the 002 plane was calculated by using Bragg's equation[24]:

$$d_{002} = \frac{\lambda}{2sin\theta}, \quad (1)$$

where, λ denotes the wavelength of Cu K_α, θ is the Bragg angle, and d_{002} refers to the interlayer spacing of the 002 plane.

The stacking height (L_c) and the crystallite size (L_a) for each sample were determined using the equations below[25]:

$$L_a = \frac{k_1\lambda}{\beta_{(100)}cos\theta}, \quad (2)$$

$$L_c = \frac{k_2\lambda}{\beta_{(002)}cos\theta}, \quad (3)$$

where, k denotes the Scherrer constant (k_1 = 1.84, k_2 = 0.94), and $\beta_{(100)}$ and $\beta_{(002)}$ are the angular widths (in radians) of peaks 100 and 002 at the half-maximum intensity, respectively.

Micromeritics ASAP 2420 instrument (N_2 adsorption-desorption isotherms at 77 K) was used for the specific surface area (SSA) of the samples, and the value was calculated based on the Brunauer–Emmett–Teller (BET) equation.

A total internal reflection Raman spectrometer (Tyrode I Raman microscope) was used to record Raman spectra. The laser wavelength was 532 nm.

X-ray photoelectron spectroscopy (XPS) was performed with a Kratos Ultra 2 Spectrometer, featuring a 500 mm Rowland circle monochromated Al Kα X-ray source, at a vacuum of 5×10^{-6} Pa.

Carbon samples were digested using a microwave-assisted acid digestion procedure with a mixture of HNO_3, HCl, H_2O_2, and HF, followed by a treatment with $HClO_4$. The digests were diluted to a final volume of 25 mL with ultrapure water and filtered through 0.45 μm membranes before analysis. Quantification was performed by inductively coupled plasma-optical emission spectroscopy (ICP-OES) at Shiyanjia using a Thermo Fisher iCAP PRO instrument.

Characterization of liquid samples

The ultimate compositions of TPO samples were also measured using the same standard as for the carbon materials.

The TPO samples were examined using gas chromatography (GC, Agilent 7890A) coupled with a mass spectrometer (MS, Agilent 5975C). The TPO samples were dissolved in a solvent mixture of dichloromethane and acetone (1:1, v/v). The GC system employed an HP-5MS column. Helium was the carrier gas at a flow rate of 1 mL/min. The GC oven temperature was set to 40 °C for 1 min for stabilization. Then, it increased at 3 °C/min to 280 °C and was held for 15 min. The split ratio was 5:1. The mass spectrometer operated within an *m/z* range of 45 to 550, and compound identification was confirmed by the NIST 11 library.

Characterization of the gas

The NCG generated during pyrolysis was monitored in real time using a micro-GC (Agilent 490 model). Four columns with thermal conductivity detectors were used to detect the amounts of N_2, H_2, O_2, CH_4, CO, CO_2, and other small hydrocarbons (C_2–C_4).

Process modeling

Mass and energy balances were based on the experimental data in this work, combined with process design and operating parameters representative of an industrial pyrolysis system developed by Envigas AB (Supplementary Fig. S2). The overall process includes the pyrolysis reactor, a carbon cooler, a condenser for pyrolysis oil and non-condensable gas, a combustion chamber for flammable-gas heat

recovery, and a boiler that converts excess heat into steam. As shown in Supplementary Fig. S3, EOL tires are continuously fed into the rotary-kiln reactor for pyrolysis. During the process, volatiles are released and partially condensed in the condenser as TPO. At the same time, the remaining NCG are headed to a combustion chamber, where they are combusted with air at a defined air-to-fuel equivalence ratio. A portion of the high-temperature flue gas is returned to the pyrolysis reactor to supply the required process heat, while the remaining fuel gas is treated as excess heat and transferred to the boiler for steam generation.

The main physical and thermochemical parameters used in the calculations are summarized in Supplementary Table S4. The calorific values of carbon and pyrolysis oil were estimated from their ultimate compositions, while the specific heat capacities of tire, carbon, and pyrolysis oil were defined based on literature and empirical correlations. A fixed thermal loss fraction was applied to represent heat dissipation through the reactor wall and associated components, consistent with industrial practice.

The combustion chamber was assumed to operate under slightly lean conditions (λ = 1.2), which is typical for NCG combustion systems to ensure complete oxidation and stable heat generation. The adiabatic flame temperature of the NCG was calculated based on the elemental composition and the defined air-to-fuel equivalence ratio, providing the reference temperature for heat recovery and energy balance estimations within the system.

Techno-economic analysis

TEA was conducted to partially evaluate the process economics, and its results were calculated based on the experimental data in this work and assumptions from a previous study[26]. A net production cost was calculated according to the TC price that provides zero loss/gain based on operating expenses alone.

Results

Pyrolysis product

The TGA result of the EOL tire was used to identify a suitable pyrolysis temperature range. As shown in Supplementary Fig. S4, the decomposition of the EOL tire started at approximately 300 °C and ended around 500 °C. Analysis of the derivative thermogravimetric (DTG) plot pointed out two well-defined decomposition peaks. The peak around 350 °C corresponds to natural-rubber decomposition, while the higher-temperature peak (450 °C) indicates the degradation of styrene-butadiene rubber (SBR)[27]. According to these curves, the pyrolysis experiments were designed to be operated at 500, 600, and 700 °C if the TC would like to keep a high fixed-carbon content.

The mass balance analysis of EOL tire pyrolysis experiments is presented in Fig. 2a. It is obvious that the yield of TC slightly decreased from 37.5% at 500 °C to 35.4% at 700 °C. A similar trend was observed in the TGA results, which confirms that the main portion of volatile components in the tire samples evaporated below 500 °C, while devolatilization above this temperature was negligible.

The yield of the TPO samples significantly decreased from 47.1% at 500 °C to 43.7% at 700 °C. This can be attributed to secondary thermal cracking reactions, where condensable vapors crack into smaller gas molecules under high-temperature conditions[28]. Consequently, the NCG yield correspondingly increased from 15.5% at 500 °C to 20.9% at 700 °C.

The chemical compounds in TPO were categorized into seven chemical groups, as shown in Fig. 2b: monocyclic aromatic hydrocarbons (MAHs), polycyclic aromatic hydrocarbons (PAHs), N-containing compounds (N-containing), S-containing compounds (S-containing), aliphatic hydrocarbons (AP), oxygenated compounds (Oxygenated), and unknown. According to the NIST 11 library, compounds with a match probability index below 80% were categorized as unknown.

Among the identified categories, aromatic hydrocarbons constituted the primary fraction of TPO. This is consistent with previous studies, as the majority of aromatics originate from the inherent structure of tire polymer precursors, particularly SBR. Aromatic rings inherent in SBR polymer chains readily depolymerize into aromatic fragments during pyrolysis[29,30]. Moreover, the percentage of aromatic compounds, particularly MAHs and PAHs, increased significantly with higher pyrolysis temperatures. The proportion of AP notably decreased, and this reduction revealed that AP underwent further cracking at elevated temperatures, transforming into smaller molecules.

Elemental levels of the TPO samples, detailed in Supplementary Table S5, revealed that carbon and hydrogen contents were around 80% and 10%, respectively, while oxygen and sulfur levels were relatively low. Such a chemical composition is closely similar to conventional crude oil, suggesting substantial commercial potential, particularly as a feedstock for further refining processes and chemical manufacturing.

The NCG were quantitatively analyzed using micro-GC. The resulting gas compositions at different temperatures are shown in Fig. 2c.

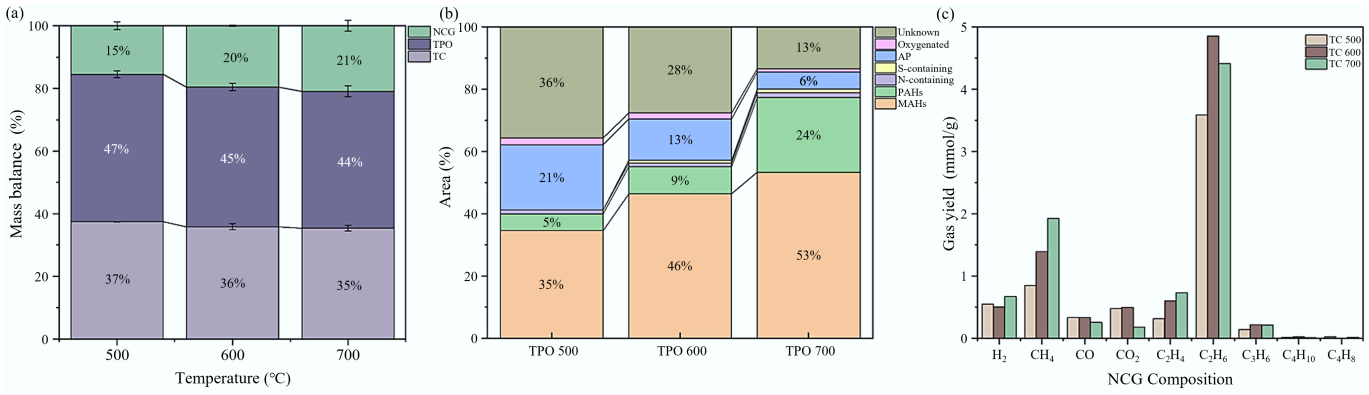

Fig. 2 Pyrolysis results of EOL tires: (**a**) mass balances of EOL tire pyrolysis experiments at 500, 600, and 700 °C; (**b**) the chemical composition groups of the TPO samples; (**c**) NCG yields of EOL tire pyrolysis experiments.

https://doi.org/10.48130/een-0026-0021

The dominant gases produced included H_2, CH_4, and C_2H_6, starting from the thermal cracking of polymer chains in SBR[31]. The yields of these gases significantly increased with rising temperature. Specifically, the yield of H_2 increased from 0.55 mmol/g at 500 °C to 0.67 mmol/g at 700 °C, and that of CH_4 from 0.85 mmol/g at 500 °C to 1.92 mmol/g at 700 °C. This clear trend demonstrated the secondary thermal cracking reaction with rising pyrolysis temperatures, which was consistent with decreased TPO yields but increased aromatic compound content.

The microstructural characteristics of the TC samples were examined by SEM, as shown in Supplementary Fig. S5. SEM images showed a blocky and porous morphology, which will be advantageous for obtaining controlled reactivity in the EAF environment. To further characterize the structural properties of TC, XRD and Raman spectroscopy analyses were performed, and their results are presented in Fig. 3a and b. The Raman spectra exhibited characteristic D-band (~1,343 cm^{-1}) and G-band (~1,589 cm^{-1}) peaks, typical of disordered or amorphous carbon materials. The I_D/I_G ratios of TC samples were calculated, and their values are above 2.4, which confirms a highly disordered carbon structure. Meanwhile, XRD patterns presented broad diffraction peaks at around 24° and 43°, which are characteristic of the (002) and (100) planes of disordered graphitic carbon. Structural parameters, including interlayer spacing (d_{002}), lateral size (L_a), and thickness (L_c) of graphitic crystallites, estimated from XRD data, are presented in Table 1. Increasing pyrolysis temperature from 500 to 700 °C led to a decrease in the d_{002} value (0.36 to 0.345 nm) and a slight increase in crystallite dimensions (L_a from 1.35 to 1.96 nm). Such changes reflect a subtle enhancement in graphitic ordering, which is likely beneficial for reducing CO_2 reactivity[32] and promoting stable slag formation in EAF applications. However, sharp peaks corresponding to impurities such as zinc sulfide (ZnS) and silica (SiO_2) at 28°, 46°, and 56° indicated notable ash and sulfur contents. Although SiO_2 and other metal oxides typically integrate safely into slag layers during steelmaking, ZnS poses significant risks to steel quality due to its sulfur contribution[32].

The SSA of the TC samples was obtained through nitrogen adsorption–desorption, as shown in Fig. 3c and Table 1. It revealed a slight decrease from 77.2 m^2/g at 500 °C to 62.5 m^2/g at 700 °C, with the pore volume first increasing from 0.18 to 0.31 cm^3/g and then decreasing to 0.13 cm^3/g. The corresponding pore size distribution plot (Fig. 3d) showed that the TC500 and TC600 contained both micropores (below 2 nm) and mesopores (between 2–50 nm)[31,33]. However, when the pyrolysis temperature increased to 700 °C (TC700), the micropores were diminished, with only mesopores distributed in the range around 2–5 nm. Although the SSA of TC was significantly lower than typical biocarbon (often exceeding 200 m^2/g)[33], these values were still above the commercial EAF carbon range (1–10 m^2/g). High SSA often correlates with increased CO_2 reactivity, which can adversely affect slag foaming stability during steelmaking[32]. This observation implied that, similar to biocarbon, additional treatments such as agglomeration may be necessary to optimize the handling and reactivity before use in the EAF process.

Elemental and ICP-OES analysis results further supported these observations, showing an increased sulfur content from 2.61% at 500 °C to 2.93% at 700 °C. However, according to EAF requirements, the sulfur content should be lower than 1%[34]. Conversely, the

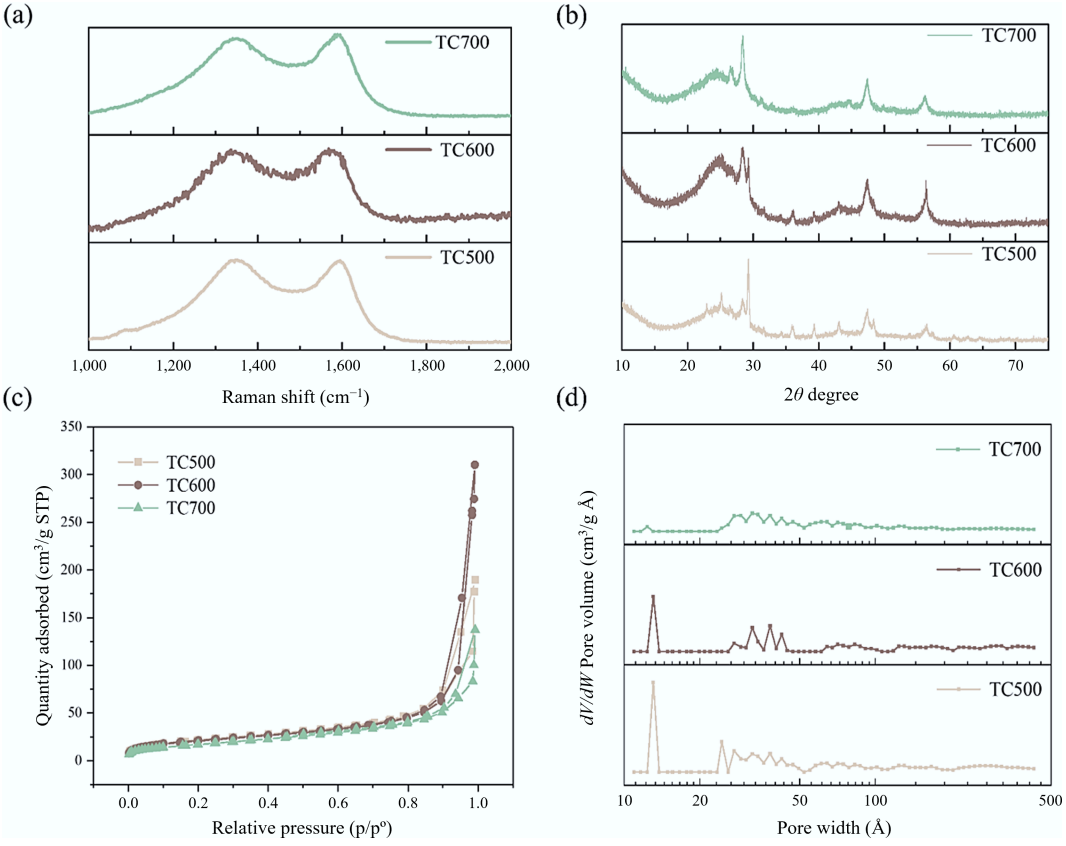

Fig. 3 Characterization of TC samples: (**a**) Raman spectra, (**b**) XRD pattern, (**c**) BET, and (**d**) pore size distribution.

Table 1 Structural properties of TC samples at different temperatures

Property	TC500	TC600	TC700
Fixed carbon (%)	67.38	82.61	81.20
Volatile matter (%)	7.98	4.14	3.01
Moisture (%)	0.13	0.34	0.25
Ash (%)	24.51	12.91	15.54
C (%)	80.07	86.4	85.8
H (%)	0.073	0.038	0.19
N (%)	0.273	0.41	0.29
S (%)	2.61	2.45	2.93
P (%)	0.044	0.047	0.019
I_D/I_G	2.43	2.66	2.61
L_a (nm)	–	1.35	1.96
L_c (nm)	–	1.14	1.02
d_{002} (nm)	0.36	0.349	0.345
SSA (m^2/g)	77.2	73.6	62.5
Pore volume (cm^3/g)	0.18	0.31	0.13

phosphorus content decreased with higher pyrolysis temperatures, and this is beneficial for EAF usage[35]. Thus, to realize the practical potential of TC in EAF applications, further desulfurization treatments were necessary.

Desulfurization of TC samples

The acid leaching after pyrolysis has been investigated for the demineralization and upgrading of recovered carbon black[22,23,36]. Therefore, the HCl/H_2O_2 treatment investigated in this work is an application-oriented adaptation of combined acid leaching and oxidative purification. The purpose was to determine whether a combined acid-oxidant treatment could reduce sulfur and other undesirable elements sufficiently for the EAF process. The high sulfur content in TC samples is primarily from organic sulfur compounds in the EOL tire[37]. During pyrolysis, these organic sulfur components decompose into sulfur-containing gases such as H_2S, COS, and CH_3SH[38]. At temperatures above 400 °C, these gases react with metal oxides commonly present in EOL tires as fillers and stabilizers, forming stable metal sulfides such as ZnS[39]. These sulfides then concentrate in the char, significantly increasing its sulfur content, as confirmed by XPS analysis[40] (Supplementary Fig. S6). Before pyrolysis, sulfur existed mainly as organic sulfur in tires (with the peak around 165 eV); however, after pyrolysis, the sulfur in the resultant TC primarily comprises inorganic forms, predominantly ZnS (with the peak around 161 eV).

Considering these findings, there are generally two primary strategies for sulfur removal from TC samples: (1) pre-pyrolysis ash removal; or (2) post-pyrolysis metal sulfide removal. Due to the intrinsic durability of tires[18], chemical treatments before pyrolysis are usually difficult and economically prohibitive. Conversely, TC is more easily processed, significantly facilitating chemical treatments and making post-pyrolysis desulfurization economically attractive. This approach, mostly using acid leaching, is already well-established for producing rCB[41].

Acid leaching treatments were applied to TC700. The desulfurization results of samples with different acid treatments are summarized in Supplementary Table S6. Acid leaching using 1 mol/L HCl and 1 mol/L acetic acid was first performed, resulting in a moderate sulfur reduction from an initial content of 2.93% down to 2.24% and 2.71%, respectively. Compared with acetic acid, the higher effectiveness of HCl can be attributed to its stronger acidity, more efficiently dissolving metal sulfides and removing ash content. Increasing the HCl concentration to 6 mol/L reduced the sulfur content in the TC sample to 1.84%. However, this sulfur content is still higher than the acceptable limit (< 1%) for carbon used in EAF steelmaking. This partial removal indicates that ZnS is relatively resistant to direct acid dissolution, following the reaction

$$ZnS + 2HCl \rightleftharpoons ZnCl_2 + H_2S.$$

The limited effectiveness was attributed to equilibrium constraints and the poor solubility of ZnS under acidic conditions alone. To enhance the desulfurization effectiveness, H_2O_2 was introduced as an oxidizing agent in combination with HCl. The addition of H_2O_2 significantly increased sulfur removal efficiency by oxidizing ZnS to more soluble zinc chloride ($ZnCl_2$) and elemental sulfur, according to

$$ZnS + 2HCl + H_2O_2 \rightarrow ZnCl_2 + S + 2H_2O.$$

After treatment with 1 mol/L HCl + H_2O_2, the sulfur content dropped dramatically to 1.28%. In the higher concentration test (6 mol/L HCl + H_2O_2), higher sulfur removal was achieved, reducing the sulfur content to 0.37%. This sulfur content met the requirement for EAF application. XPS analysis of these chemically treated TC samples (Supplementary Fig. S6) also confirmed that the ZnS peak at ~161 eV nearly disappeared after acid leaching, leaving only a small amount of thiophenic sulfur (~164 eV). This highly purified sample was termed TC700-A, which was derived from the TC700 sample after desulfurization.

Further ICP-OES analysis results of impurities before and after desulfurization are shown in Supplementary Table S7. The desulfurization in this work notably reduced impurities: Zn, Fe, Ca, Al, and P. Most significantly, the zinc content decreased substantially from 4.399% to 0.118%, clearly proving successful ZnS removal. Moreover, phosphorus content decreased from 0.019% to 0.009%, meeting the usage standards of commercial EAF carbon.

Subsequently, the structure of TC700-A was thoroughly compared with EAF carbon and biocarbon materials. Raman spectroscopy (Fig. 4a) showed similar broad D-band peaks in both TC and commercial EAF carbon, characterized by high I_D/I_G ratios of approximately 2.96 and 2.80, respectively. These values are indicative of amorphous carbon structures. In contrast, biocarbon showed a slightly ordered structure with a lower I_D/I_G ratio (2.50).

XRD patterns in Fig. 4b showed that the TC sample and EAF carbon exhibited similar XRD profiles, particularly the distinct (002) graphite peak around 25°, corresponding to d_{002} around 0.36 nm. This contrasted with the broader and shifted peak (around 23°) of biocarbon, resulting in a higher d_{002} spacing (0.39 nm). Correspondingly, crystallite sizes (L_a and L_c) of TC700-A (3.62, 1.37 nm) and EAF carbon (2.87, 1.42 nm) were similar, markedly larger than TC700 (1.96, 1.02 nm), suggesting comparable thermal stability and reduced reactivity toward CO_2, beneficial for slag foaming stability in EAF processes. It also confirmed the complete removal of ZnS impurities in the desulfurization process, because of the disappearance of ZnS-associated diffraction peaks compared with TC700.

As shown in Table 2, in addition, TC demonstrated better properties compared with the commercial EAF carbon, including a higher fixed-carbon content (85.33% vs 67.80%), lower ash (9.7% vs 30.92%), and significantly reduced sulfur (0.37% vs 1.02%). Such attributes improve both the efficiency and quality of steel produced using this material. Compared with biocarbon, TC700-A offered substantial advantages, particularly lower phosphorus content (0.009% vs 0.017%) and a significantly reduced specific surface area (79.1 vs 394 m^2/g), implying lower reactivity toward CO_2.

TGA under O_2 and CO_2 atmospheres further corroborated these findings, as shown in Fig. 4c and d. Compared with commercial EAF carbon, both biocarbon and TC exhibited higher reactivity. This difference arises primarily from morphological variations, as shown

https://doi.org/10.48130/een-0026-0021

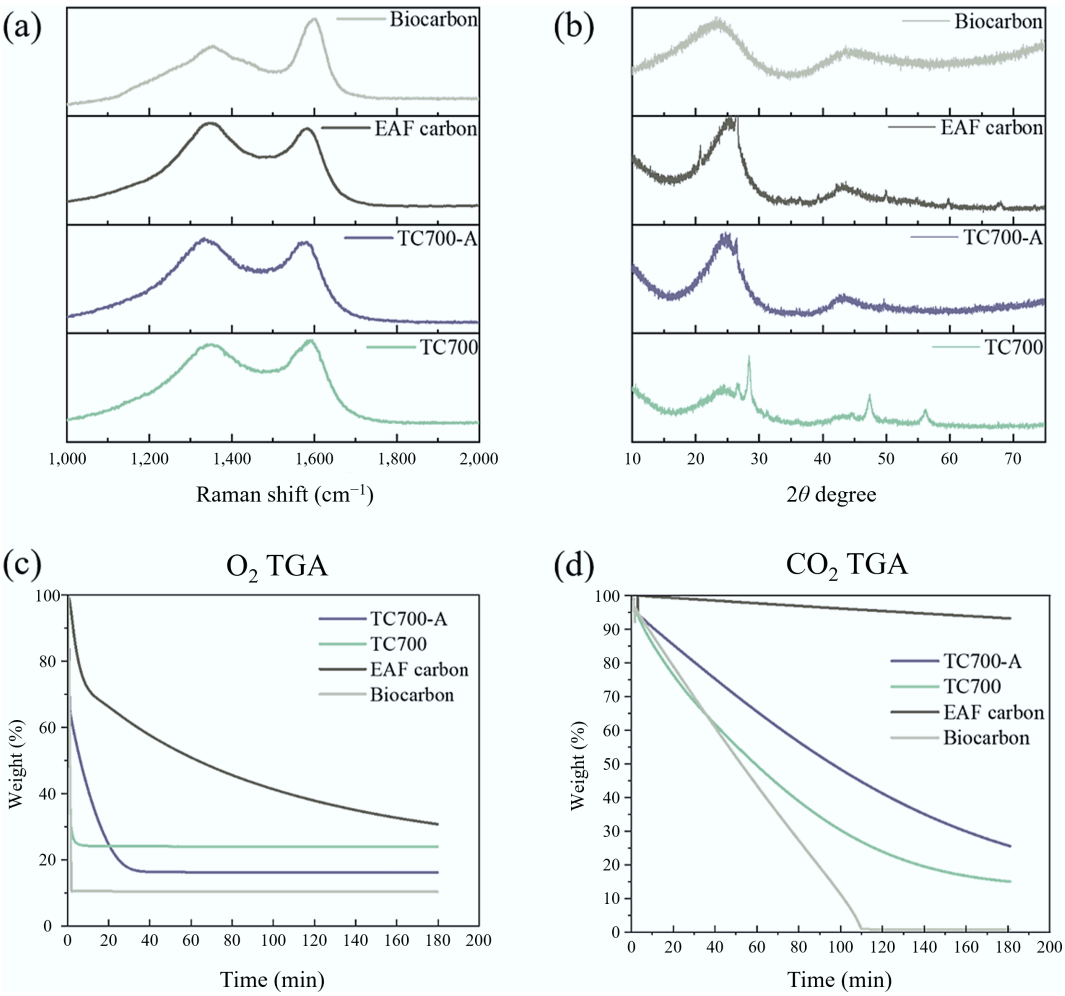

Fig. 4 Characterization of desulfurized TC samples: (**a**) Raman spectra; (**b**) XRD spectra; (**c**) O_2-TGA results; (**d**) CO_2-TGA results.

in Supplementary Fig. S7. Firstly, the commercial EAF carbon occurred as hard lumps; biocarbon largely retained its original particulate structure but generated substantial fines under collision or compression, whereas TC was friable and readily converted to powder. Secondly, EAF carbon had a much lower SSA value (7.48) compared with TC700-A (79.1) and biocarbon (394). Therefore, these factors greatly reduce gas-solid contact with O_2 and CO_2, thereby suppressing the reactivity of EAF carbon. Prior studies also indicated that agglomeration can improve morphology and SSA, with the potential to enhance the reactivity of both biocarbon and TC[12]. Finally, at the microcrystalline level, the commercial EAF carbon showed larger crystallite sizes, more stacked graphene layers (L_c = 1.42), and smaller interlayer spacings, indicating a more graphitic structure with higher thermal stability and slower reaction kinetics.

Table 2 Properties of carbon for EAF steelmaking

Property	TC700-A	EAF carbon	Biocarbon
Fixed carbon (wt.%)	85.33	67.80	88.50
Volatile matter (wt.%)	4.62	1.25	9.62
Moisture (wt.%)	0.35	0.03	0.63
Ash (wt.%)	9.7	30.92	1.25
C (wt.%)	89.3	85.52	88.71
H (wt.%)	0.15	0.33	2.09
N (wt.%)	–	1.51	0.34
S (wt.%)	0.37	1.02	0
P (wt.%)	0.009	0.006	0.017
I_D/I_G	2.96	2.8	2.5
L_a (nm)	3.62	2.87	2.07
L_c (nm)	1.37	1.42	0.73
d_{002} (nm)	0.363	0.357	0.39
SSA (m^2/g)	79.1	7.48	394

Although there remained a gap relative to the commercial EAF carbon, TC700-A was less reactive than biocarbon. In CO_2-TGA, biocarbon was fully consumed after ~110 min, whereas TC continued to react; it is shown that TC700-A maintained a slower, more controlled carbon consumption. Such moderated reactivity is crucial for stable furnace operation, efficient slag foaming, and improved energy efficiency in EAF steelmaking[42]. Overall, these results demonstrated that desulfurized TC has strong potential as an ACS for EAF steelmaking.

TEA of TC for EAF steelmaking

To evaluate the practical feasibility and economic competitiveness of TC as an ACS for EAF steelmaking, a comprehensive analysis was conducted. The TEA model employed in this study was validated using experimental data from this work. The process simulation framework was based on a realistic industrial scenario where the produced NCG was combusted directly to supply heat required for the pyrolysis process itself, representing typical commercial-scale pyrolysis plants.

The energy flows associated with the EOL tire pyrolysis process are illustrated using a Sankey diagram in Fig. 5a, clearly including energy inputs, outputs, and internal energy recycling. All energy balances in the Sankey diagram were normalized with a feed rate of 1.25 tons/h of EOL tire feedstock. This corresponds to an annual throughput of approximately 10,000 t. The transport distance was set to 750 km, reflecting the actual distance between Stena AB and Envigas.

As depicted, the only external energy input to the system was the chemical energy contained in the EOL tire feedstock, supplemented by heat supplied through the combustion of NCG to sustain the pyrolysis operation. The process outputs included the chemical and sensible heat contents of the resulting pyrolysis products (TC, TPO, and NCG), along with heat losses. Based on the mass and energy balances, the heat requirement of the pyrolysis process is approximately 0.64 MW, while NCG combustion generates about 2.29 MW of thermal energy, of which approximately 1.96 MW is available as usable heat. A portion of this heat is returned to the pyrolysis reactor in the form of high-temperature flue gas, directly supplying the thermal demand of the pyrolysis process. The remaining flue gas is directed to the boiler unit, where excess thermal energy is recovered and converted into hot steam, with the exhaust gas finally released at approximately 130 °C. As a result, the external energy input required for the pyrolysis operation is fully compensated by the combustion of internally generated NCG, leading to an essentially energy-self-sufficient process. In addition, the recovered excess heat is converted into hot steam with an output of approximately 1.32 MW, which is treated as a useful byproduct of the system.

Moreover, the latent chemical heat remaining within the TC and TPO presents additional opportunities for recovery and utilization in adjunct processes, potentially further enhancing overall energy efficiency and reducing operational costs.

To provide a clear insight into the economic attractiveness of TC, a detailed TEA was carried out. The key economic parameters are summarized in Tables 3–6. To account for potential differences in feedstock composition and its impact on equipment durability, the assumed reactor lifetime for tire pyrolysis was set to 10 years, compared with 15 years for biocarbon pyrolysis[26]. This adjustment reflects possible corrosion and maintenance effects associated with higher sulfur and ash contents in waste tires. Detailed assessment of capital investment and equipment wear will be carried out in future work once pilot-scale operational data are available.

As shown in Tables 5 and 6, the production cost of TC, calculated without considering revenues from TPO, is 2,425 SEK/ton of EOL tires processed, corresponding to 6,930 SEK/ton of TC. This cost level is substantially lower than the reported production cost of biocarbon, which typically exceeds 15,000 SEK/ton, highlighting the intrinsic economic advantage of TC production[48]. In the base-case scenario adopted here, EOL tires were assigned zero cost because they are commonly treated as a waste stream within established collection and recycling systems[43]. In contrast, biomass feedstocks such as wood pellets show significantly higher market prices (above 4,000 SEK/ton[49]), driven by competing demand from energy production, activated carbon manufacturing, battery electrode materials, and other industrial applications[50]. Additionally, biomass availability tends to be seasonal and geographically constrained, leading to higher logistical complexity and associated costs[51]. In contrast, EOL tires are consistently available year-round, supported by mature and centralized collection infrastructures and established recycling systems in many regions globally[52]. The yield of TC is another critical economic advantage. The carbon yield from EOL tires (approximately 35%) is considerably higher than biocarbon (approximately 25%)[26], leading to greater production efficiency and economic benefit per unit of input feedstock.

Despite this advantage over biocarbon, the baseline production cost of TC remains higher than the current market price of commercial EAF carbon, which is approximately 1,000 SEK/ton[53]. Therefore, while TC is economically favorable relative to other alternative carbon sources, further cost reduction or revenue integration is required for TC to be directly competitive with fossil-based EAF carbon on a price basis.

To evaluate the feasibility of TC as a direct replacement for EAF carbon, an alternative economic scenario was assessed in which the selling price of TC is assumed to be equal to the market price of EAF carbon (1,000 SEK/ton). The analysis (Table 6) indicates that, at a TC price of 1,000 SEK/ton, a minimum TPO revenue of 2,075 SEK/ton for EOL tires is required for the system to reach break-even operation. This corresponds to a minimum TPO selling price of 4.72 SEK/kg.

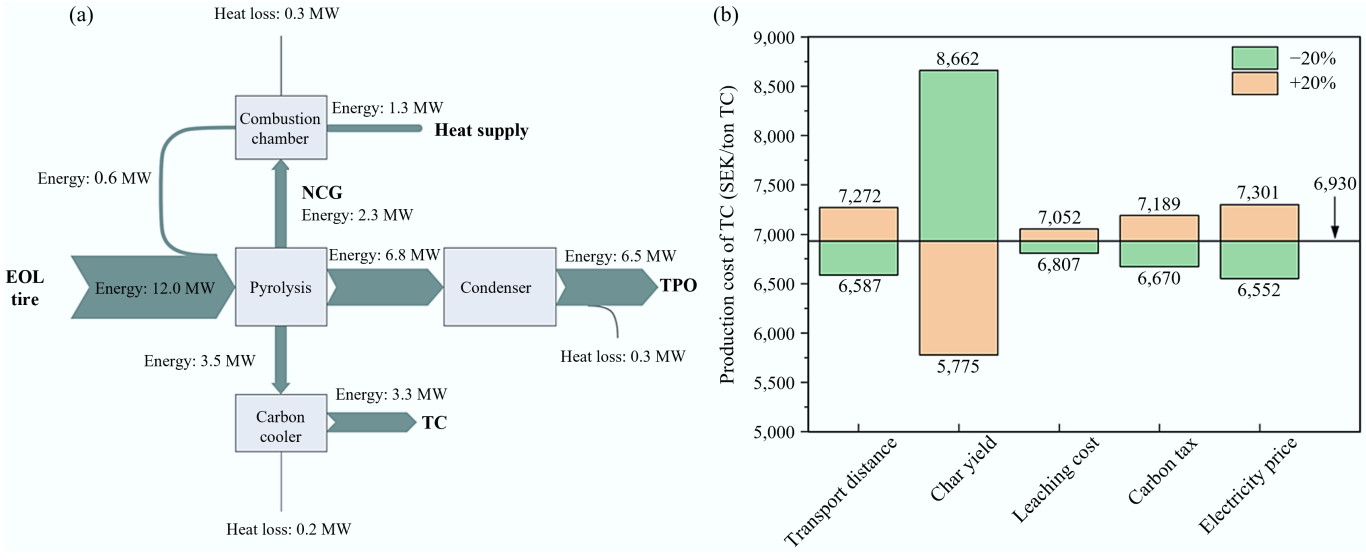

Fig. 5 (**a**) Energy balance of EOL tire pyrolysis process; (**b**) sensitivity study on the production cost of TC (SEK/ton TC).

https://doi.org/10.48130/een-0026-0021

Table 3 The parameters and the reference for the TEA analysis of TC production

Parameter	Assumption	Ref.
Transport distance	750 km	Envigas AB
Transport cost	0.8 SEK/ton EOL tire/km	Envigas AB
Feedstock cost	0 SEK/ton	Envigas AB[43]
Capital cost	30,000,000 SEK	Envigas AB
Plant lifetime	10 years	Envigas AB
Plant annual capacity	10,000 tons EOL tire/year	Envigas AB
Salary and overhead	11,000,000 SEK/year	[26]
Electricity cost	1.09 SEK/kWh	[44]
TPO selling price	6 SEK/kg	[45]
Heat selling price	0.85 SEK/kWh	[46]
H_2O_2 price	6.26 SEK/L	Marketing price
HCl price	0.66 SEK/L	Marketing price
H_2O_2 usage	25.41 L/ton EOL tire	Experimental data
HCl usage	83.3 L/ton EOL tire	Experimental data
Carbon tax	775 SEK/ton CO_2	[47]

Table 4 The parameters of the main process used in the TEA calculations

Parameters in the main process	Value
Plant annual capacity	10,000 tons/year
TC yield	35%
TPO yield	44%
Carbon content in TC	81%
Heat production from NCG	1.056 MWh/ton EOL tire
Energy consumption	600 kWh/ton EOL tire
CO_2 emission	0.587 ton CO_2/ton EOL tire

Notably, this value is close to the low end of the current market price range for TPO (4.5–7.2 SEK/kg in Europe[45,54]), which means that the proposed pricing strategy is commercially feasible under realistic market conditions. This demonstrates that TC can be economically competitive with EAF carbon through integrated valorization of TPO, while simultaneously enabling waste utilization and carbon substitution. Consequently, the combined production and sales strategy presents a promising and economically robust pathway for replacing fossil-based EAF carbon with TC in EAF steelmaking.

In the previous base-case assumption, the cost of EOL tires was taken as zero because they are generally treated as a waste stream. However, this assumption may not apply universally. Under some market conditions, EOL tire scrap may carry a purchase cost of approximately 20–30 USD/ton, which is consistent with prices for shredded tire-derived fuel in decent market conditions[55], corresponding to an average of about 228 SEK/ton. When this feedstock cost is included, the production cost of TC increases from 6,930 to approximately 7,580 SEK/ton TC. Although this is slightly higher than the base-case estimate, it remains substantially lower than the reported production cost of biocarbon.

In addition to feedstock cost, the TEA results are influenced by local utility prices, process design, and consumables market conditions. In particular, the assumed electricity price, production yield, and transportation distance may vary considerably between locations and operating conditions. A sensitivity analysis shown in Fig. 5b was conducted to evaluate the effect of variations in key parameters on the production cost of TC. The parameters studied included transport distance, char yield, leaching cost, carbon tax, and electricity price. Among these, the char yield showed the greatest influence on the production cost of TC, followed by electricity price and transport distance, while leaching cost showed the least sensitivity.

Table 5 The cost/revenue in the TEA analysis

Cost/revenue	Values
Transportation cost	600 SEK/ton EOL tire
Capital cost	1,400 SEK/ton EOL tire
Energy cost	654 SEK/ton EOL tire
Leaching cost	214 SEK/ton EOL tire
Carbon tax	455 SEK/ton EOL tire
Sale of heat	−897 SEK/ton EOL tire
Total cost	2,425 SEK/ton EOL tire (6,930 SEK/ton TC)

Table 6 Price analysis of byproducts from TC production

	Price/assumption
Assumed price of TC	350 SEK/ton EOL tire (1,000 SEK/ton TC)
Minimum revenue from TPO	2,075 SEK/ton EOL tire
Minimum TPO selling price	4.72 SEK/kg

In conclusion, TEA clearly indicates that TC offers substantial economic advantages over commercial EAF carbon and biocarbon in EAF steelmaking. However, the TEA presented here should be interpreted as a scenario-based preliminary assessment rather than a definitive commercial evaluation. While the results indicate promising economic potential for TC, the final production cost will depend on site-specific feedstock contracts, utility prices, heat utilization opportunities, and the market value of byproducts.

Discussion

The pyrolysis and desulfurization experiments in this study demonstrated that EOL tires can be effectively transformed into a carbonaceous material suitable for steelmaking. In EAF steelmaking, carbonaceous materials fulfill several metallurgical and operational functions. They are fed into the furnace to: (i) supply carbon for carburization of molten steel; (ii) promote slag foaming by reacting with FeO in the slag to generate CO gas; (iii) provide a reducing environment to prevent excessive FeO formation; and (iv) serve as an energy source through partial oxidation. The performance of a carbon source in EAF operations is therefore governed by its fixed-carbon content, reactivity toward CO_2 and O_2, ash composition, and impurity levels such as S and P. The relatively ordered carbon microstructure and low SSA of TC700-A indicate a controlled CO_2 and O_2 reactivity, ensuring a stable and sustained gas production rate during slag foaming. Entirely reactive materials, like biocarbon, tend to cause over-foaming and operational instability, whereas overly inert coke limits slag formation. The balanced reactivity of TC700-A therefore supports optimized foaming behaviour, contributing to efficient heat transfer and reducing electrical energy consumption in the EAF. Moreover, compared with EAF carbon, the significantly lower sulfur content minimizes the risk of contamination in the melt process. This can ensure compatibility with high-quality steel production standards. In comparison with other alternative carbon sources explored in previous studies, TC meets the fundamental structural and compositional requirements for potential direct use in EAF applications, as does biocarbon.

TEA corroborated the technical findings and demonstrated that TC can be produced at a substantially lower cost than biocarbon, due to minor feedstock costs and higher carbon yields. The baseline production cost of TC was estimated at 2,425 SEK/ton of EOL tires (corresponding to 6,930 SEK/ton of TC). This is significantly lower than the reported cost of biocarbon but still higher than that of commercial EAF carbon. However, if TC is evaluated within an

integrated production system, the byproduct TPO provides an effective pathway to achieve more price competitiveness. Scenario analysis showed that, by pricing TC at the level of EAF carbon (1,000 SEK/ton), the system can reach economic break-even provided that TPO is sold at a minimum price of 4.72 SEK/kg, which is within the reported market range, slightly above the lower bound. This demonstrates that TC can competitively replace fossil-based EAF carbon through realistic and commercially feasible by-product revenue strategies. Combined with near energy self-sufficiency, reduced reliance on fossil-based carbon, and compatibility with existing EAF operations, these results position TC as a promising and economically viable alternative carbon source for sustainable steelmaking.

Future work

This study demonstrated the laboratory-scale potential of producing TC through pyrolysis and HCl/H_2O_2 desulfurization, resulting in structural and compositional characteristics comparable to those of conventional EAF carbon and biocarbon. Based on the above, the next stage of research will focus on exploring the pilot-scale validation and the development of the product to make it suitable for industrial application.

In this study, TC700-A still exhibits a higher SSA than EAF carbon; therefore, further investigation into subsequent agglomeration and densification is required to ensure its mechanical properties approach those of EAF carbon. Additionally, it is necessary to determine its bulk density, compressive strength, flowability, pore structure, and O_2/CO_2 reactivity. After that, the optimized agglomerates will be evaluated in pilot-scale EAF trials with industrial partners. These trials can supply experimental data to determine whether agglomeration or binder addition is required for charging or pneumatic injection. It will also assess carbon utilization efficiency, injection stability, slag-foaming behavior, dust generation, reaction kinetics, and operational energy requirements under realistic furnace conditions. Particular attention will be given to balancing sufficient mechanical integrity with controlled carbon availability and ensuring that the selected binder does not introduce undesirable sulfur, phosphorus, volatile matter, or excessive ash.

The life-cycle assessment is the next step and will be conducted to quantify the environmental benefits and potential trade-offs associated with the large-scale implementation of TC as a fossil carbon substitute in EAF steelmaking.

In addition, future work will also explore system-level integration between tire pyrolysis and EAF processes, focusing on recovering and reusing non-condensable gas or waste heat for feedstock preheating and off-gas treatment. This integration could enhance the total energy efficiency, reduce emissions, and promote circularity across the steel value chain.

Conclusions

This study systematically assessed the potential of TC as a sustainable ACS for EAF steelmaking. TC was produced through pyrolysis at 500–700 °C. Although the untreated material exhibited high sulfur levels due to the presence of ZnS, a simple HCl/H_2O_2 purification step effectively reduced the sulfur content to 0.37 wt.% and lowered other harmful impurities such as phosphorus, thereby meeting the requirements for EAF operation. Comprehensive comparative analyses confirmed that desulfurized TC exhibited high fixed-carbon content, moderate reactivity, and structural similarities to EAF carbon, which is advantageous for stable slag formation and controlled carbon consumption in EAF operations.

TEA showed that TC has a clear economic advantage over biocarbon, mainly due to its lower feedstock cost and higher carbon yield. Under the base-case assumptions, the production cost of TC was estimated to be lower than that of biocarbon, although still higher than the market price of commercial EAF carbon. When revenues from TPO are included, TC may achieve price competitiveness with EAF carbon under favorable market conditions. Overall, these results indicate that desulfurized TC is a promising alternative carbon source for EAF steelmaking from both material and economic perspectives.

Supplementary information

It accompanies this paper at: https://doi.org/10.48130/een-0026-0021

Ethical statements

During the preparation of this manuscript, the authors used OpenAI Codex solely for English-language editing and polishing. The tool was not used to generate scientific content, analyze data, interpret results, or prepare figures. The authors reviewed and verified all AI-assisted revisions, and take full responsibility for the accuracy, integrity, and originality of the final manuscript. No AI tool is credited as an author.

Author contributions

The authors confirm their contributions to the paper as follows: Yanghao Jin: conceptualization, investigation, methodology, formal analysis, writing – original draft; Yazhe Wang: conceptualization, investigation, methodology, formal analysis, writing – original draft; Zexuan Li: investigation, methodology, formal analysis; Samina Gulshan: investigation, formal analysis, resources, writing – review & editing; Tong Han: investigation, formal analysis, resources, writing – review & editing; Aekjuthon Phounglamcheik: investigation, formal analysis, resources, writing – review & editing; Konstantinos Rigas: investigation, formal analysis, resources, writing – review & editing; Ziyi Shi: conceptualization, validation, formal analysis, visualization, writing – review & editing; Pär G. Jönsson: writing – review & editing, supervision; Weihong Yang: writing – review & editing, supervision, project administration, funding acquisition. All authors reviewed the results and approved the final version of the manuscript.

Data availability

All data generated or analyzed during this study are included in this published article and its supplementary information files.

Acknowledgments

We thank Envigas AB, Outokumpu Europe Oy, Ovako Sweden AB, and Stena Recycling AB for providing materials and for the valuable discussions that greatly contributed to this work.

Funding

The authors gratefully acknowledge financial support from VINNOVA, the Swedish Innovation Agency (project number 2024-02656).

https://doi.org/10.48130/een-0026-0021

Declarations

Competing interests

The authors declare that they have no known competing financial interests or personal relationships that could have appeared to influence the work reported in this paper.

Author details

[1]Department of Materials Science and Engineering, KTH Royal Institute of Technology, Stockholm 100 44, Sweden; [2]Envigas AB, Torshamnsgatan 27, Kista 164 40, Sweden

References

[1] IEA. 2020. *Steel technology roadmap*. www.iea.org/reports/iron-and-steel-technology-roadmap

[2] Rumsa M, John M, Biswas W. 2025. Global steel decarbonisation roadmaps: near-zero by 2050. *Environmental Impact Assessment Review* 112:107807

[3] Kim J, Son M, Park J, Kim J. 2022. Optimized rotary hearth furnace utilization with blast furnace and electric arc furnace: techno-economics, CO_2 reduction. *Fuel Processing Technology* 237:107450

[4] Lee G, Son M, Bae J, Kim J, Han J. 2025. Model-based life cycle assessment of steelmaking: role of solid waste recycling via rotary hearth furnace in South Korea. *Journal of Cleaner Production* 527:146687

[5] Mokrzycki E, Gawlik L. 2024. Decarbonisation determinants of the steel industry. *Gospodarka Surowcami Mineralnymi – Mineral Resources Management* 40:71–90

[6] Lu YC, Liang W, Karasev A, Wang G, Wang C. 2025. Toward fossil-free steelmaking: overview of physiochemical properties of hydrochar and its application in blast furnace and electric arc furnace processes. *cScience* 1:e70004

[7] Echterhof T. 2021. Review on the use of alternative carbon sources in EAF steelmaking. *Metals* 11:222

[8] DiGiovanni C, Li D, Ng KW, Huang X. 2025. Evaluation of biochar and coke blends for slag foaming applications in electric arc furnace steelmaking. *Steel Research International* 96:2400518

[9] Kieush L, Schenk J, Koveria A, Rantitsch G, Hrubiak A, et al. 2023. Utilization of renewable carbon in electric arc furnace-based steel production: comparative evaluation of properties of conventional and non-conventional carbon-bearing sources. *Metals* 13:722

[10] Gul E, Riva L, Nielsen HK, Yang H, Zhou H, et al. 2021. Substitution of coke with pelletized biocarbon in the European and Chinese steel industries: an LCA analysis. *Applied Energy* 304:117644

[11] Cardarelli A, Barbanera M. 2023. Substitution of fossil coal with hydrochar from agricultural waste in the electric arc furnace steel industry: a comprehensive life cycle analysis. *Energies* 16:5686

[12] Demus T, Reichel T, Schulten M, Echterhof T, Pfeifer H. 2016. Increasing the sustainability of steel production in the electric arc furnace by substituting fossil coal with biochar agglomerates. *Ironmaking & Steelmaking* 43:564–570

[13] Robinson R, Brabie L, Pettersson M, Amovic M, Ljunggren R. 2022. An empirical comparative study of renewable biochar and fossil carbon as carburizer in steelmaking. *ISIJ International* 62:2522–2528

[14] DiGiovanni C, Echterhof T. 2024. Progress toward biocarbon utilization in electric arc furnace steelmaking: current status and future prospects. *Journal of Sustainable Metallurgy* 10:2047–2067

[15] Roy P, Rodriguez-Uribe A, Mohanty AK, Pujari D, Tiessen M, et al. 2024. Production cost of biocarbon and biocomposite, and their prospects in sustainable biobased industries. *Sustainability* 16:5633

[16] Liu Z, Wang S, Ouyang Y. 2017. Reliable biomass supply chain design under feedstock seasonality and probabilistic facility disruptions. *Energies* 10:1895

[17] Mohanty AK, Vivekanandhan S, Das O, Romero Millán LM, Klinghoffer NB, et al. 2024. Biocarbon materials. *Nature Reviews Methods Primers* 4:19

[18] Xiao Z, Pramanik A, Basak AK, Prakash C, Shankar S. 2022. Material recovery and recycling of waste tyres - a review. *Cleaner Materials* 5:100115

[19] Palos R, Gutiérrez A, Vela FJ, Olazar M, Arandes JM, et al. 2021. Waste refinery: the valorization of waste plastics and end-of-life tires in refinery units. A review. *Energy & Fuels* 35:3529–3557

[20] Torretta V, Rada EC, Ragazzi M, Trulli E, Istrate IA, et al. 2015. Treatment and disposal of tyres: two EU approaches. A review. *Waste Management* 45:152–160

[21] Ahmad S, Ahmad M, Naeem K, Humayun M, Sebt-E-Zaeem S, et al. 2016. Oxidative desulfurization of tire pyrolysis oil. *Chemical Industry and Chemical Engineering Quarterly* 22:249–254

[22] Martínez JD, Cardona-Uribe N, Murillo R, García T, López JM. 2019. Carbon black recovery from waste tire pyrolysis by demineralization: production and application in rubber compounding. *Waste Management* 85:574–584

[23] Jiang G, Pan J, Deng W, Sun Y, Guo J, et al. 2022. Recovery of high pure pyrolytic carbon black from waste tires by dual acid treatment. *Journal of Cleaner Production* 374:133893

[24] Pope CG. 1997. X-ray diffraction and the Bragg equation. *Journal of Chemical Education* 74:129

[25] Cao H, Li K, Zhang H, Liu Q. 2023. Investigation on the mineral catalytic graphitization of anthracite during series high temperature treatment. *Minerals* 13:749

[26] Zaini IN, Sophonrat N, Sjöblom K, Yang W. 2021. Creating values from biomass pyrolysis in Sweden: co-production of H_2, biocarbon and bio-oil. *Processes* 9:415

[27] Kumaravel ST, Murugesan A, Kumaravel A. 2016. Tyre pyrolysis oil as an alternative fuel for diesel engines – a review. *Renewable and Sustainable Energy Reviews* 60:1678–1685

[28] Martínez JD, Puy N, Murillo R, García T, Navarro MV, et al. 2013. Waste tyre pyrolysis – a review. *Renewable and Sustainable Energy Reviews* 23:179–213

[29] Jerzak W, Wądrzyk M, Sieradzka M, Magdziarz A. 2024. Valorisation of tyre waste from a vulcanisation plant by catalytic pyrolysis – experimental investigations using pyrolysis–gas chromatography–mass spectrometry and drop-tube–fixed-bed reactor. *Energy Conversion and Management* 313:118642

[30] Berrueco C, Esperanza E, Mastral FJ, Ceamanos J, García-Bacaicoa P. 2005. Pyrolysis of waste tyres in an atmospheric static-bed batch reactor: analysis of the gases obtained. *Journal of Analytical and Applied Pyrolysis* 74:245–253

[31] Li Z, Tao L, Yang Q, Chen L, Qi H, et al. 2023. Mechanism research on hydrogen production from catalytic pyrolysis of waste tire rubber. *Fuel* 331:125846

[32] Tian H, Hu Q, Wang J, Chen D, Yang Y, et al. 2021. Kinetic study on the CO_2 gasification of biochar derived from *Miscanthus* at different processing conditions. *Energy* 217:119341

[33] Chowdhury ZZ, Karim MZ, Ashraf MA, Khalid K. 2016. Influence of carbonization temperature on physicochemical properties of biochar derived from slow pyrolysis of durian wood (*Durio zibethinus*) sawdust. *BioResources* 11:3356–3372

[34] Metal Zenith. 2025. *Coke: essential fuel and reducing agent in steelmaking processes*. https://metalzenith.com/blogs/steel-production-processing-terms/coke-essential-fuel-and-reducing-agent-in-steelmaking-processes?utm_source=chatgpt.com

[35] Yamasue E, Matsubae K. 2019. Phosphorus in steelmaking processes. In *Phosphorus Recovery and Recycling*, eds Ohtake H, Tsuneda S. Singapore: Springer. pp. 349–364 doi: 10.1007/978-981-10-8031-9_24

[36] Cardona-Uribe N, Betancur M, Martínez JD. 2021. Towards the chemical upgrading of the recovered carbon black derived from pyrolysis of end-of-life tires. *Sustainable Materials and Technologies* 28:e00287

[37] Cheng Z, Li M, Li J, Lin F, Ma W, et al. 2021. Transformation of nitrogen, sulfur and chlorine during waste tire pyrolysis. *Journal of Analytical and Applied Pyrolysis* 153:104987

[38] Zhang X, Tang J, Chen J. 2022. Behavior of sulfur during pyrolysis of waste tires: a critical review. *Journal of the Energy Institute* 102:302–314

[39] Lanteigne JR, Laviolette JP, Chaouki J. 2015. Behavior of sulfur during the pyrolysis of tires. *Energy & Fuels* 29:763−774
[40] Zhang J, Zhu M, Jones I, Okoye CO, Zhang Z, et al. 2021. The transformation and fate of sulphur during CO_2 gasification of a spent tyre pyrolysis char. *Proceedings of the Combustion Institute* 38:3891−3898
[41] Bowles AJ, Wilson AL, Fowler GD. 2023. Synergistic benefits of recovered carbon black demineralisation for tyre recycling. *Resources, Conservation and Recycling* 198:107124
[42] Kieush L, Schenk J, Koveria A, Hrubiak A, Hopfinger H, et al. 2023. Evaluation of slag foaming behavior using renewable carbon sources in electric arc furnace-based steel production. *Energies* 16:4673
[43] Laghezza M, Papari S, Fiore S, Berruti F. 2023. Techno-economic assessment of the pyrolysis of rubber waste. *Energy* 278:127841
[44] Eurostat. 2026. *Electricity prices for industrial consumers - bi-annual data (from 2007 onwards)*. https://ec.europa.eu/eurostat/databrowser/product/view/nrg_pc_205
[45] Kibria MA, Thomas BS, Bhattacharya M, Bhattacharya S. 2024. Processing of metal-free end-of-life tyres (EOLTs) to fuels and products: an experimental study with process simulation and economic analysis from an Australian perspective. *Clean Technologies and Environmental Policy* 26:4215−4229
[46] Egüez A. 2021. District heating network ownership and prices: the case of an unregulated natural monopoly. *Utilities Policy* 72:101252
[47] Martinsson G, Sajtos L, Strömberg P, Thomann C. 2024. The effect of carbon pricing on firm emissions: evidence from the Swedish CO_2 tax. *The Review of Financial Studies* 37:1848−1886
[48] Bergman R, Sahoo K, Englund K, Mousavi-Avval SH. 2022. Lifecycle assessment and techno-economic analysis of biochar pellet production from forest residues and field application. *Energies* 15:1559
[49] Pinho R, Oliveira M, Teixeira BMM, da Silva Borges AD. 2025. Evaluating quality and price dynamics of wood pellets in the Portuguese market: Impacts of geopolitical and economic factors. *Energy Strategy Reviews* 59:101719
[50] Xie Y, Wang L, Li H, Westholm LJ, Carvalho L, et al. 2022. A critical review on production, modification and utilization of biochar. *Journal of Analytical and Applied Pyrolysis* 161:105405
[51] Malladi KT, Sowlati T. 2018. Biomass logistics: a review of important features, optimization modeling and the new trends. *Renewable and Sustainable Energy Reviews* 94:587−599
[52] Valentini F, Pegoretti A. 2022. End-of-life options of tyres. A review. *Advanced Industrial and Engineering Polymer Research* 5:203−213
[53] Salimbeni A, Lombardi G, Rizzo AM, Chiaramonti D. 2023. Techno-Economic feasibility of integrating biomass slow pyrolysis in an EAF steelmaking site: a case study. *Applied Energy* 339:120991
[54] Al Yahya S, Omar MM. 2024. Technoeconomic analysis: the potential and opportunities of transforming Saudi Arabian scrap tires into synthetic fuel via vacuum pyrolysis. *Frontiers in Energy Research* 12:1415901
[55] Xin C, Liu J, Chen T, Chen H, Huo H, et al. 2025. Technical and economic analysis of a novel integrated energy system with waste tire pyrolysis and biogas. *Processes* 13:415

Copyright: © 2026 by the author(s). Published by Maximum Academic Press, Fayetteville, GA. This article is an open access article distributed under Creative Commons Attribution License (CC BY 4.0), visit https://creativecommons.org/licenses/by/4.0/.